Received: 13 September 2018 | Revised: 20 December 2018 | Accepted: 26 December 2018
DOI: 10.1002/rcm.8389

RESEARCH ARTICLE

WILEY Rapid Communications in Mass Spectrometry

An automated laser fluorination technique for high-precision analysis of three oxygen isotopes in silicates

Nak Kyu Kim[1] | Minoru Kusakabe[2] | Changkun Park[3] | Jong Ik Lee[1] | Keisuke Nagao[3] | Yuma Enokido[4] | Shigeru Yamashita[5] | Sun Young Park[3]

[1] Unit of Antarctic K-route Expedition, Korea Polar Research Institute, Incheon 21990, Republic of Korea

[2] Department of Environmental Biology and Chemistry, University of Toyama, Toyama 930-8555, Japan

[3] Division of Earth-System Sciences, Korea Polar Research Institute, Incheon 21990, Republic of Korea

[4] Division of Earth and Planetary Material Science, Tohoku University, Sendai, Miyagi 980-8578, Japan

[5] Institute for Planetary Materials, Okayama University, Misasa, Tottori 682-0193, Japan

Correspondence
Nak Kyu Kim, Unit of Antarctic K-route Expedition, Korea Polar Research Institute, 26 Songdomirae-ro, Yeonsu-gu, Incheon 21990, South Korea.
Email: kimnk@kopri.re.kr

Funding information
Korea Polar Research Institute, Grant/Award Number: PM18030 (20140409) and PE18110

Rationale: The three oxygen isotopes in terrestrial/extraterrestrial silicates can provide geochemical and cosmochemical information about their origin and secondary processes that result from isotopic exchange. A laser fluorination technique has been widely used to extract oxygen from silicates for $\delta^{17}O$ and $\delta^{18}O$ measurements by isotope ratio mass spectrometry. Continued improvement of the techniques is still important for high-precision measurement of oxygen-isotopic ratios.

Methods: We adopted an *automated lasing technique* to obtain reproducible fluorination of silicates using a CO_2 laser-BrF_5 fluorination system connected online to an isotope ratio mass spectrometer. The automated lasing technique enables us to perform high-precision analysis of the three oxygen isotopes of typical reference materials (e.g., UWG2 garnet, NBS28 quartz and San Carlos olivine) and in-house references (mid-ocean ridge basalt glass and obsidian). The technique uses a built-in application of laser control with which the laser power can be varied in a programmed manner with a defocused beam which is in a fixed position.

Results: The oxygen isotope ratios of some international reference materials analyzed by the manual lasing technique were found to be isotopically lighter with wider variations in $\delta^{18}O$ values, whereas those measured by the automated lasing technique gave better reproducibility (less than 0.2‰, 2SD). The $\Delta^{17}O$ values, an excess of the $\delta^{17}O$ value relative to the fractionation line, also showed high reproducibility (±0.02‰, 2SD).

Conclusions: The system described herein provides high-precision $\delta^{17}O$ and $\delta^{18}O$ measurements of silicate materials. The use of the automated lasing technique followed by careful and controlled purification procedures is preferred to achieve satisfactory isotopic ratio results.

1 | INTRODUCTION

In 1963, Clayton and Mayeda[1] published a paper on the application of bromine pentafluoride (BrF_5) as a fluorination reagent for the extraction of oxygen from silicate and oxide minerals using a nickel tube with external heating for oxygen isotope analysis. After their historical paper, fluorination-with-laser-heating methods have been developed such as those reported by Sharp,[2] Elsenheimer and Valley,[3] Miller et al,[4] Kusakabe et al,[5] Pack et al,[6] Ahn et al,[7] and Tanaka and Nakamura.[8] However, the methods of isotopic analysis are different. The results obtained for a given sample by different authors vary substantially, and there is still disagreement among the reported isotopic data of reference minerals. This is caused by fractionation during extraction procedures adopted in each laser fluorination technique. The possible causes of the variability include (1) the type of laser used, e.g., infrared CO_2 (wavelength of 10.6 μm)

or Nd:YAG (1064 nm) lasers[3] (2) laser irradiation conditions, e.g., beam diameter and increase rate of output power;[8-10] (3) fluorinating agent (F_2 or BrF_5) and its purity;[11,12] (4) sample size;[10,13] and (5) design of the sample holder.[14] It is worth emphasizing that fluorination and purification procedures require caution to prevent possible isotopic fractionation during such procedures.

In this study, we describe an infrared CO_2 laser-BrF_5 fluorination system for the analysis of three oxygen isotopes in silicates. We used an automated laser control for lasing silicates in the BrF_5 atmosphere. We measured the three oxygen isotope compositions of five silicate samples; garnet standard at University of Wisconsin (UWG2 garnet), National Bureau of Standard quartz (NBS28 quartz), San Carlos olivine, Juan de Fuca oceanic basalt (JFB) glass, and obsidian as an in-house silicate standard from Coso volcanic field, California, USA, using our improved methods.

2 | SYSTEM DESCRIPTION

The three oxygen isotope analytical system for silicates using a CO_2 laser-BrF_5 fluorination at the Korea Polar Research Institute (KOPRI, Incheon, Republic of Korea) was installed in 2007 and has been used for the measurement of the oxygen isotopes of terrestrial and extraterrestrial rocks and minerals.[7,15-17] Recently, the system has been replaced completely, with a new metal vacuum line for O_2 extraction and purification. A new mass spectrometer was also introduced. The principle of the system is the same as that described in previous studies.[2,5,7] The laser fluorination system consists of five components (Figure 1); (1) BrF_5 storage and recovery, (2) reaction chamber for laser fluorination, (3) CO_2 laser, (4) purification line, and (5) a gas source isotope ratio mass spectrometer (MAT 253 plus, Thermo Fisher Scientific, Bremen, Germany). BrF_5 is used as the fluorination reagent. A moderate quantity of BrF_5 is purified by a consecutive freeze-pump-thaw method and transferred into a reagent reservoir made of polychlorotrifluoroethylene (PCTFE called Kel-F®). The reaction chamber made of stainless steel is sealed by a BaF_2 window (5 mm thick, 50 mm diameter) with a Kalrez® O-ring (Figure 2A). The whole reaction chamber is mounted on a motorized X-Y stage and placed under a CO_2 infrared (10.6 μm wavelength) laser system (Universal Laser Systems, Scottsdale, AZ, USA). The laser output power can be adjusted from 0 to 100% of the maximum output of 25 W using a computer control program built into the laser unit. The purification line is made of stainless-steel tubing (SUS316) and metal bellows-sealed valves (SS-4H, Swagelok®, Solon, OH, USA). Oxygen transfer and the elimination of impurity gases are monitored by Pirani gauges. The extracted oxygen gas is collected in a glass cryogenic trap that contains a pellet of 13X molecular sieve (trap 3, Figure 1). After desorption of O_2, the gas pressure is measured using a pressure transducer. Calibration of the pressure transducer will be briefly described later.

3 | ANALYTICAL METHODS

3.1 | Laser fluorination and gas purification

Several coarse- or fine-grained silicate samples weighing approximately 2 mg were loaded in a nickel sample holder (Figure 2B), which was placed in the reaction chamber (Figure 2A). The chamber is assembled with the purification line using a metal gasket (VCR®, Swagelok®), and then evacuated to 10^{-3} mbar or better. At the beginning it is heated to 150°C overnight in vacuum with an external heating

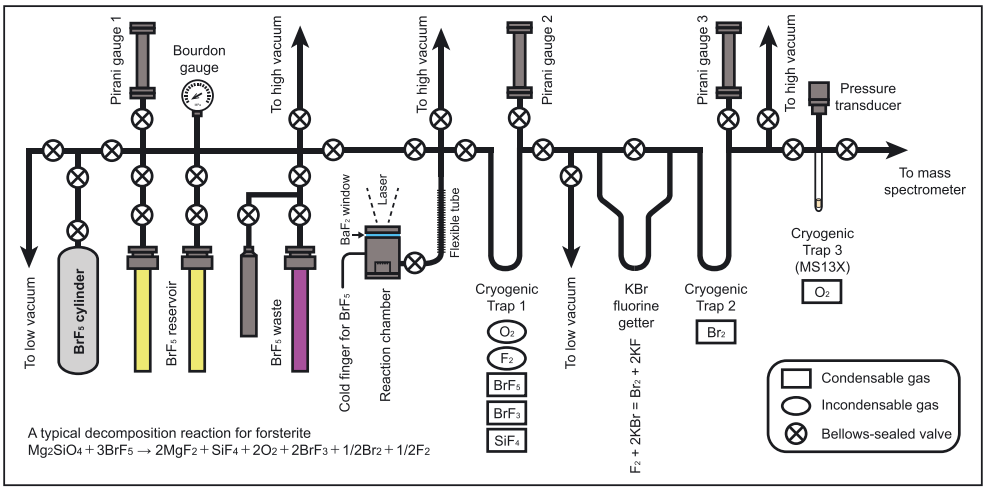

FIGURE 1 Schematic diagram of the laser fluorination line. Silicates and oxide minerals are heated by a CO_2-laser in the presence of BrF_5 in the reaction chamber. After the reaction, the excess BrF_5 and product gases such as O_2, F_2, BrF_3, SiF_4, etc., pass through the purification line. The condensable gases are removed in the first cryogenic traps. Fluorine, which is an incondensable gas at liquid nitrogen temperature (−196°C), reacts with KBr to produce bromine. After that, bromine is trapped in a second cryogenic trap. The purified oxygen gas is collected in the third cryotrap containing a pellet of 13X molecular sieve (MS13X). The gas pressure of the oxygen released from MS13X at room temperature is measured by a pressure transducer to calculate the oxygen yield. The oxygen gas is expanded into the sample bellows of the dual-inlet system of the isotope ratio mass spectrometer for measuring the oxygen isotope ratios [Color figure can be viewed at wileyonlinelibrary.com]

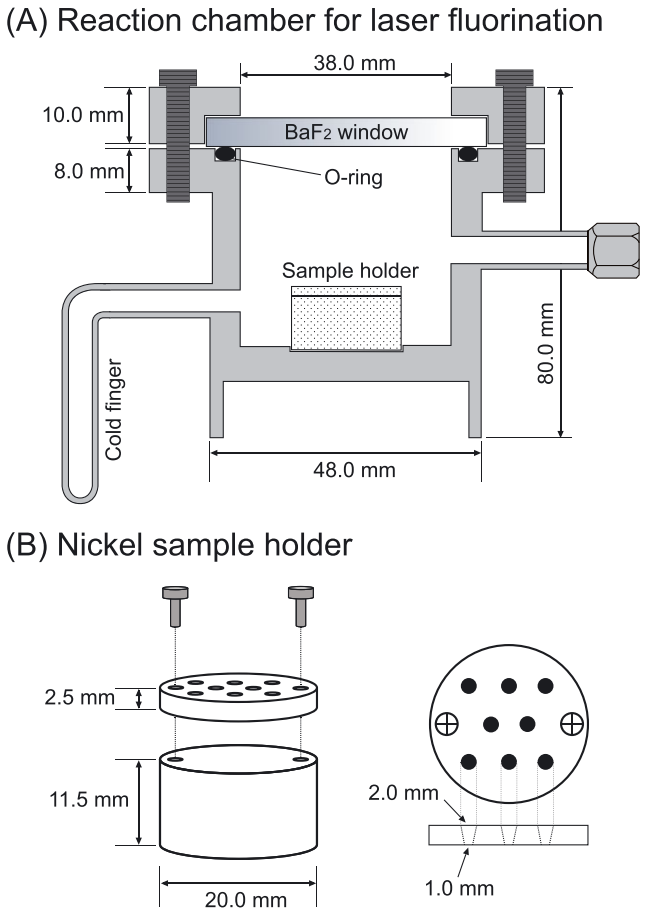

FIGURE 2 Schematic diagram of A, reaction chamber and B, nickel sample holder with dimensions. The sample holder consists of top and bottom parts. The top part has eight tapered (cone-shaped) holes having an upper diameter of 2 mm and a lower diameter of 1 mm. It is fixed on the bottom holder by two screws. This sample holder design is advantageous for washing and cleaning after an experiment. The sample holder filled with approximately 2 mg of the sample on each hole is placed in the reaction chamber made of stainless steel, and the reaction chamber is then sealed by a transparent BaF_2 window with a Kalrez O-ring [Color figure can be viewed at wileyonlinelibrary.com]

jacket to remove adsorbed atmospheric moisture. Before sample analysis, a small amount of BrF_5 gas is introduced into the reaction chamber for pre-fluorination for 1 h at room temperature to remove the remaining moisture adsorbed on the surface of the samples and metal inside the chamber. Prior to laser fluorination, all the remaining gases in the chamber are thoroughly evacuated (<10^{-4} mbar). Then, approximately 110 mbar of BrF_5 is introduced into the reaction chamber using an attached cold finger (Figure 2A). The amount of introduced BrF_5 is roughly two times greater than the stoichiometric requirement of a ~2 mg silicate sample. We adopted two modes of laser power control for fluorination; manual mode and automated (Table 1). In the manual lasing mode, the laser output and positioning of the laser beam are manually adjusted, whereas in the automated lasing technique the position of laser beam is fixed and the diameter of laser beam and laser power are changed using the laser control functions in the laser system. At the beginning of operation in the

TABLE 1 Mode of laser power control for fluorination

Power control mode	Beam size[a] (mm)	Reaction time[b] (min)	Laser power[c] (%)	Additional lasing[d]
Manual mode	<0.5	~10	3 → 70	-
Automated mode I	>3.0	2–5	20 → 60	2–5 min in manual mode
Automated mode II	>2.5	2–5	10 → 60	
Automated mode III	>2.0	2–5	5 → 60	

[a]Beam sizes were checked by burning and melting test of wood and aluminum plates.

[b]The end of reaction was decided by there being no more glow in the sample holder.

[c]Generally, the initial laser power in the automated mode is increased as the beam size is reduced.

[d]Additional lasing with focused beam applied to ensure complete reaction. Completion of the reaction was decided by watching for no more glow in the sample holder.

automated mode, the sample is gradually heated at low laser power followed by gradual increase to 60%. Usually, most of the samples are decomposed at the end of the automated lasing mode. After the fluorination, unreacted grains, if remaining, are heated by reducing the beam size to ~0.5 mm to complete the fluorination. The end of the reaction is decided by observing no further glow on a monitor connected to a CCD camera. This additional laser heating is performed on the sample fragments hidden at the edge of the sample holder.

All gaseous species from a sample are expanded into the first cryogenic trap to remove condensable gases such as excess BrF_5, BrF_3 and SiF_4 at liquid nitrogen temperature (−196°C) for 7 min (Figure 1). Non-condensable F_2 gas, if any, is then allowed to pass through the KBr getter heated at 150°C in order to convert it into bromine ($F_2 + 2KBr \rightarrow Br_2 + 2KF$) which is trapped in the second cryogenic trap 2 for 5 min. The resulting pure O_2 is finally collected on cryogenic trap 3 containing a pellet of 13X molecular sieve (MS13X) for 15 min at liquid nitrogen temperature (Figure 1). The oxygen yield is calculated from the O_2 gas pressure measured with a pressure transducer after desorption of the O_2 gas from the MS13X trap at room temperature. The volume of the cryogenic trap 3 and pressure transducer are calibrated using a known amount of CO_2 before attaching the transducer to the line. For the calibration the pellet of 13X molecular sieve in trap 3 is removed, as molecular sieve is known to adsorb CO_2 irreversibly. During a series of extraction and purification procedures, the line is maintained at approximately 40°C using heating tapes to minimize adsorption of gases on the inner wall of the metallic line.

3.2 | Mass spectrometer and conditions for oxygen isotope measurement

The gas source isotope ratio mass spectrometer equipped with a dual-inlet system is connected on-line to the laser fluorination system (Figure 1). In our system, oxygen gas (O_2) is used as the analyte. The

oxygen gas desorbed from the MS13X in cryogenic trap 3 is expanded into a metal bellows in the dual-inlet system directly. For the $^{17}O/^{16}O$ and $^{18}O/^{16}O$ ratio analysis, we determine the beam intensity of the masses 32, 33, and 34 collected by Faraday cups connected to the resistors with $\Omega = 3 \times 10^8$, 3×10^{11}, and 1×10^{11}, respectively. Isodat 3.0 software (Thermo Fisher Scientific) is used for data acquisition. Each measurement consisted of 10 cycles with an integration time of 26 s. The internal precision of $\delta^{17}O$ measurements is <0.02‰ (2SEM, standard error of the mean). The data shown in this paper is an average of duplicate measurements.

To check daily systematic bias and operating conditions of the mass spectrometer, so-called zero-enrichment analysis is performed by introducing the working standard O_2 gas into both the sample and the reference bellows prior to the sample measurements. The zero-enrichment measurements typically showed less than 0.03‰ change in the $\delta^{17}O$ and $\delta^{18}O$ values, so we did not take the instrumental bias into consideration in later data handling. If a sample contains nitrogen compounds, fluorination may produce NF_3 and the NF^+ fragment ion (*m/z* 33) forms in the ion source, overlapping the $^{17}O^{16}O^+$ peak in the mass spectrum because the mass resolution of ~200 of the mass spectrometer is much lower than the required resolution of ~4440 ($M/\Delta M$) for the separation of $^{16}O^{17}O^+$ from $^{14}N^{19}F^+$. To obtain a precise $^{17}O/^{16}O$ ratio of a natural sample, this isobaric interference at *m/z* 33 must be considered.[4] Thus, we checked for the presence of $^{14}N^{19}F_2^+$ and $^{14}N^{19}F_3^+$ peaks at *m/z* 52 and *m/z* 71 after each analysis. The oxygen gases extracted from typical silicate minerals, however, showed no recognizable peaks at these masses, indicating that their interference was negligible. In the case where samples contain a large amount of nitrogen, the interference of $^{14}N^{19}F^+$ can be problematic.[12]

3.3 | Determination of δ-values for working standard O_2

The oxygen isotope ratios are generally expressed in δ-notation relative to VSMOW (Vienna Standard Mean Ocean Water) where δ is defined as the per mil (‰) deviation of $^{17}O/^{16}O$ and $^{18}O/^{16}O$ ratios of a sample from those of VSMOW, i.e., $\delta^{17}O = \{(^{17}O/^{16}O)_{sample}/(^{17}O/^{16}O)_{VSMOW}\} - 1$ and $\delta^{18}O = \{(^{18}O/^{16}O)_{sample}/(^{18}O/^{16}O)_{VSMOW}\} - 1$. However, we report both values relative to our 'working standard O_2 (WST)' reference gas due to there being no direct calibration for the reference gas relative to VSMOW in this study (Table 2).

In an oxygen three-isotope plot, if the range of $\delta^{17}O$ and $\delta^{18}O$ values is large, the values do not fall on a straight line but on a slightly convex curve.[18] Therefore, $\Delta^{17}O$, the deviation of $^{17}O/^{16}O$ ratios of samples from the fractionation line, is defined by a linear equation as $\Delta^{17}O = \delta'^{17}O - \lambda \times \delta'^{18}O - \gamma$, where $\delta'^{17}O = 10^3\ln(1 + \delta^{17}O)$ and $\delta'^{18}O = 10^3\ln(1 + \delta^{18}O)$, λ is a slope of mass-dependent fractionation line, and γ is the ordinate offset of the fractionation line.[18] To compare the deviation of $^{17}O/^{16}O$ ratios of the reference samples

TABLE 2 $\delta^{17}O$, $\delta^{18}O$ and $\Delta^{17}O$ values of the reference samples obtained in automated and manual lasing modes

			$\delta^{17}O_{WST}$[a]			$\delta^{18}O_{WST}$[a]			$\Delta^{17}O$[b]			$\delta^{18}O_{VSMOW}$[c]
Sample	Lasing technique	No. of analyses	Avg. (‰)	SD (2σ)	SEM (2σ)	Avg. (‰)	SD (2σ)	SEM (2σ)	Avg. (‰)	SD (2σ)	SEM (2σ)	Avg. (‰)
Juan de Fuca	Automated III	6	8.006	0.079	0.032	15.340	0.168	0.069	0.001	0.016	0.007	5.593
Basalt glass	Automated II	3	8.000	0.110	0.064	15.326	0.231	0.134	0.002	0.011	0.006	5.579
	Automated I	36	8.017	0.105	0.018	15.353	0.195	0.033	0.005	0.020	0.003	5.606
	Manual	39	7.884	0.245	0.039	15.130	0.428	0.069	−0.010	0.047	0.008	5.384
UWG2 garnet	Automated III	17	8.129	0.059	0.014	15.579	0.094	0.023	−0.001	0.020	0.005	5.829
	Automated II	3	8.117	0.019	0.011	15.569	0.047	0.027	−0.008	0.009	0.005	5.820
	Automated I	4	8.145	0.049	0.024	15.586	0.043	0.022	0.011	0.027	0.013	5.836
	Manual	12	8.099	0.121	0.035	15.441	0.189	0.055	0.041	0.065	0.019	5.693
NBS28 quartz	Automated III	10	10.007	0.074	0.024	19.143	0.139	0.044	0.011	0.019	0.006	9.359
	Automated I	7	9.881	0.071	0.027	18.901	0.124	0.047	0.010	0.016	0.006	9.120
	Manual	10	9.620	0.212	0.067	18.423	0.379	0.120	0.000	0.020	0.006	8.646
San Carlos olivine	Automated III	9	7.946	0.093	0.031	15.200	0.161	0.054	0.014	0.021	0.007	5.455
	Automated I	6	7.834	0.056	0.023	14.981	0.125	0.051	0.017	0.026	0.010	5.238
	Manual	10	7.876	0.099	0.031	15.070	0.193	0.061	0.012	0.016	0.005	5.326
Obsidian	Automated III	20	9.528	0.094	0.021	18.252	0.166	0.037	−0.002	0.025	0.006	8.477
(in-house)	Automated II	2	9.516	0.021	0.015	18.212	0.095	0.067	0.006	0.028	0.020	8.437
	Automated I	6	9.500	0.023	0.009	18.190	0.042	0.017	0.002	0.017	0.007	8.415

[a]δ-values are expressed as a per mil relative to working standard O_2 (WST).

[b]$\Delta^{17}O = 10^3\ln(\delta^{17}O_{WST} + 1) - 0.528 \times 10^3\ln(\delta^{18}O_{WST} + 1) + 0.065$.

[c]$\delta^{18}O$ values relative to VSMOW are converted from the $\delta^{18}O$ values relative to the working standard O_2 by a conversion factor of 0.9904 (n = 24) by assuming $\delta^{18}O_{VSMOW}$ = 5.8‰ for UWG2 garnet.[29]

SD = standard deviation; SEM = standard error of the mean

in this study, we report $\Delta^{17}O$ values of the samples relative to UWG2 garnet. First, we defined the fractionation line for silicate materials from the regression of the $\delta'^{17}O_{WST}$ and $\delta'^{18}O_{WST}$ values in this study (Figure S1, supporting information). The regression equation is expressed as $\delta'^{17}O_{WST} = (0.528 \pm 0.002) \times \delta'^{18}O_{WST} - (0.057 \pm 0.034)$. The slope of 0.528 is in good agreement with those from other studies on terrestrial rocks and minerals.[19-23] The $\Delta^{17}O$ values are calculated from $\delta'^{18}O_{WST}$ and $\delta'^{17}O_{WST}$ values and by assuming that $\Delta^{17}O$ value of UWG2 garnet ($n = 24$) is zero, where $\lambda = 0.528$ and $\gamma = -0.065$. However, this approach can be used only for relative comparison of the samples in oxygen isotope analysis because we cannot assure that the oxygen isotope ratios of UWG2 garnet plot exactly on the fractionation line on the VSMOW scale. Furthermore, the slope of the fractionation line assigned by a measurement of terrestrial samples displays little difference among the sample collections.[19-23]

4 | RESULTS AND DISCUSSION

We repetitively analyzed the reference minerals to assess the analytical reproducibility. The results are summarized in Table 2. The individual $\delta^{18}O$ values of the reference materials are shown in Figures 3A–3D, where the data obtained in different analytical modes are grouped. The results of 200 individual oxygen isotope ratio measurements and the relevant analytical parameters (e.g., sample weight, oxygen yield, lasing mode, beam size, and reaction time) are given in the Table S1 (supporting information). In the following discussion, the reproducibility of the average $\delta^{17}O$ and $\delta^{18}O$ values is expressed as 2SD (2 times the standard deviation) unless mentioned otherwise.

The previous laser fluorination system at KOPRI used a 20 W CO_2 laser with binocular optical system to observe the reaction.[7] The reaction chamber was manipulated manually on the XY-stage during laser irradiation with a highly focused beam. The analytical reproducibilities for the $\delta^{18}O$ values of typical reference minerals such as UWG2 garnet, NBS28 quartz, San Carlos olivine and JFB glass (in-house standard sample at that time) were ± 0.21‰, ±0.29‰, ±0.18‰ and ± 0.25‰, respectively.[7] Following the modification of the purification line with a new 25 W CO_2 laser, we re-analyzed the same reference materials using the manual lasing mode which was the same as previously reported. The results neither reached a sufficient level of reproducibility nor were they in agreement with the recommended values (Figure 3). In particular, the JFB glass that has been used as our in-house reference showed a large isotopic variation. We initially thought

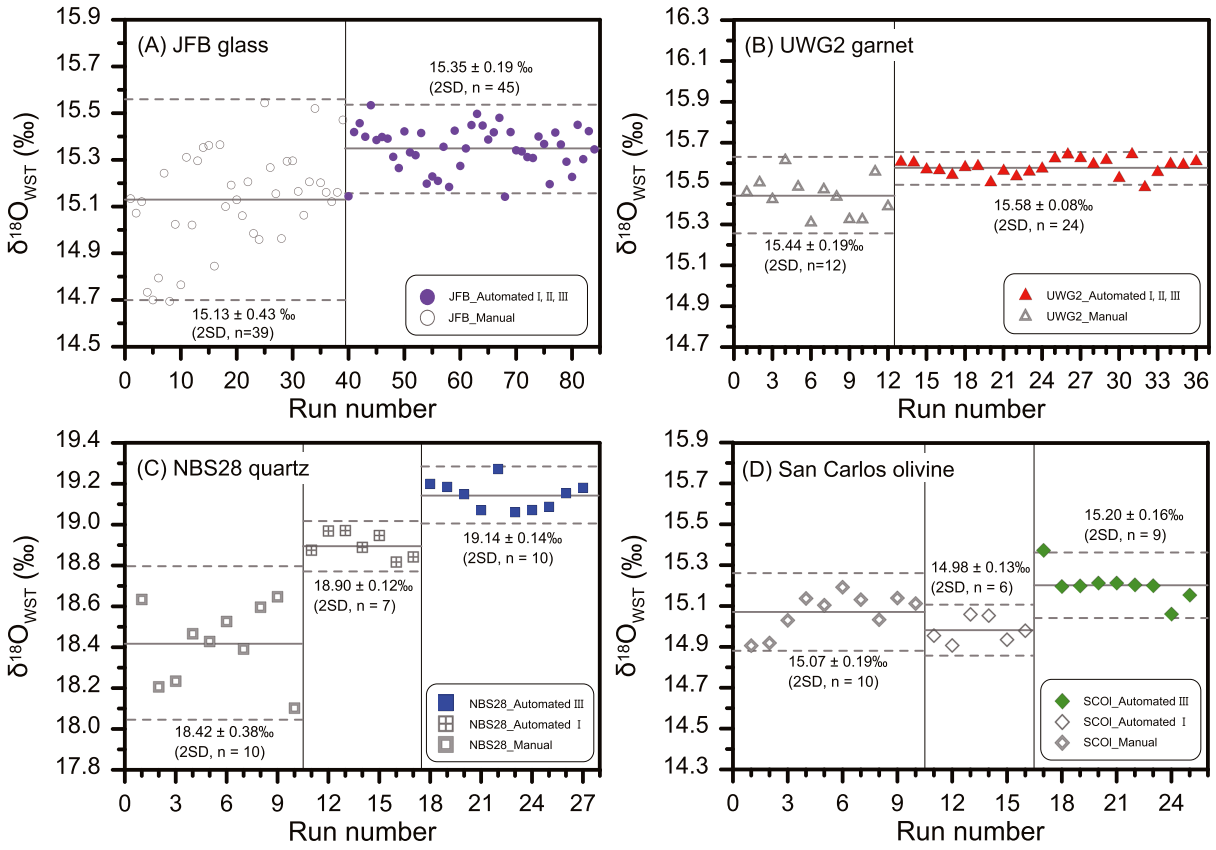

FIGURE 3 Deviations of A, Juan de Fuca basalt (JFB) glass, B, UWG2 garnet, C, NBS28 quartz, and D, San Carlos olivine measurements by manual and automated laser techniques. Errors (2σ) are within the size of the symbols in the plots. Averages are shown as gray solid lines and 2σ standard deviations (SD) are shown as gray dashed lines. The automated lasing technique provides better precision than the manual lasing technique. Moreover, the quartz and olivine results obtained by the automated lasing technique are grouped by the size of the laser beam [Color figure can be viewed at wileyonlinelibrary.com]

that the variation resulted from the presence of numerous olivine and plagioclase micro-phenocrysts because uneven distribution of the phenocrysts could have caused isotopic fractionation in the glass fragments (Figure S2, supporting information).[24] However, it was found that such micrometer-sized phenocrysts in the basalt glass do not affect the oxygen isotope variability (Table S2, supporting information). Instead we observed that the results of JFB glass obtained by the manual lasing technique can be grouped depending on who handled the laser system (Figure S3, supporting information); obvious operator bias was found. For this reason, we have introduced the automated lasing technique to minimize any unpredictable human error. The advantage of automated lasing is that a sample is irradiated uniformly using a defocused beam that covers the entire sample without changing the laser beam position (Table 1). The maximum diameter of the defocused beam used here was about 3 mm in the case of automated mode I. However, it proved difficult to react the sample completely with the 3 mm diameter beam due to the laser having too low an energy density. An oversized laser beam could influence samples in the neighboring holes. The minimum diameter of the defocused beam applied to our sample holder was 2 mm (automated mode III). We also tested an intermediately sized beam (2.5 mm diameter, automated mode II) to check if the isotopic fractionation depends on the beam size. We used a maximum laser power of up to 60% during the automated lasing modes to prevent the BaF_2 window from cracking.

The three sub-methods of the automated lasing technique (automated modes I, II and III) were first applied to JFB glass, UWG2 garnet and obsidian to see whether the different energy density of the laser affects the isotopic results. These three materials did not show significant difference in the $\delta^{18}O$ values obtained by the three automated lasing techniques (see Figures 3A and 3B, and Table 2). Thus, we decided to adopt automated mode III for further analyses. After adopting this technique, the reproducibility of all measurements was improved. It is noted that $\delta^{18}O$ values of all tested samples increased consistently compared with the results obtained using the manual mode (Figure 3). However, the NBS28 quartz exhibited large variations in the $\delta^{18}O$ value depending on the laser irradiation techniques (Figure 3C). It is known that 10.6 μm-wavelength irradiation is well absorbed by quartz.[2,10] Figure 3C shows that this mineral exhibited low $\delta^{18}O$ values with poor reproducibility when analyzed using the manual mode or low-density laser beam. The poor reproducibility was probably caused by either grain sputtering during lasing[10,13] or preferential vaporization of SiO_2. Isotopic fractionation is associated with partial vaporization of SiO_2 molecules when they are irradiated at low temperatures.[9,25]

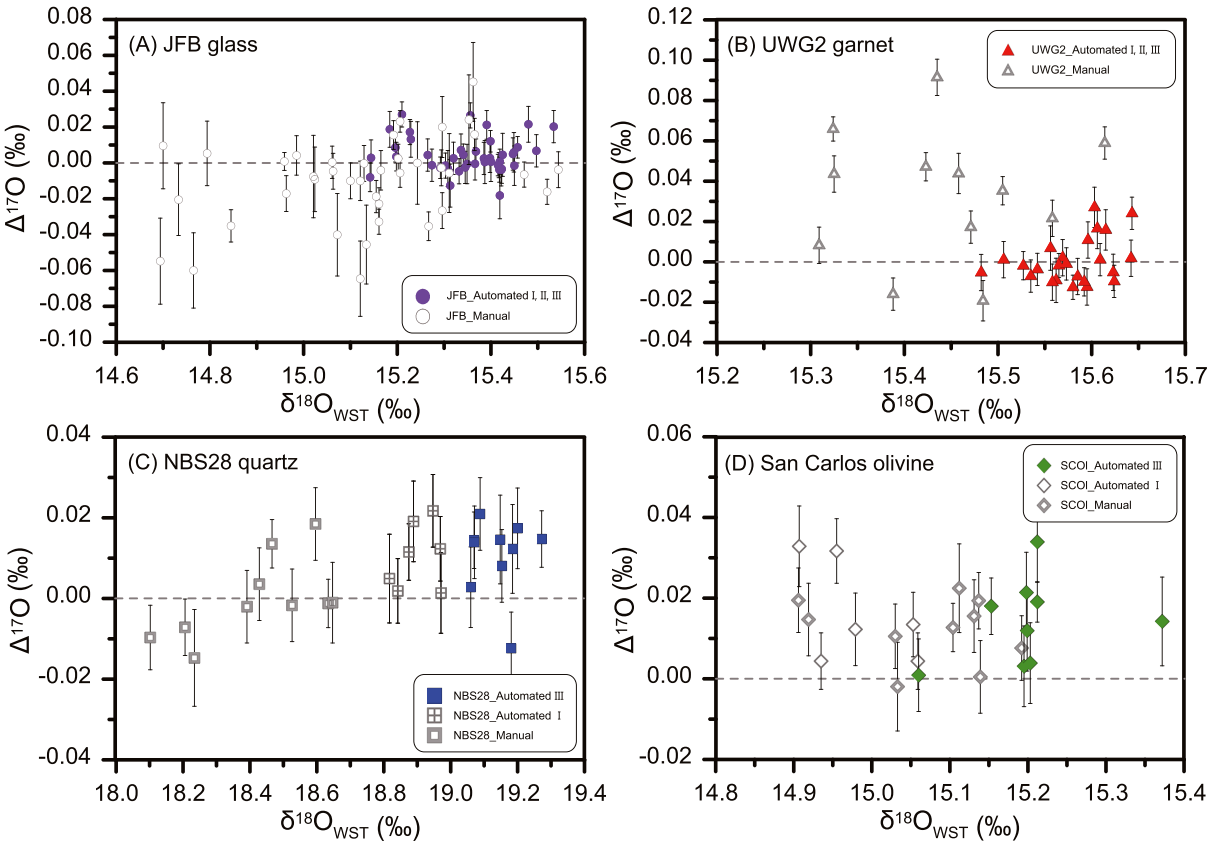

FIGURE 4 $\Delta^{17}O$ values of A, Juan de Fuca basalt (JFB) glass, B, UWG2 garnet, C, NBS28 quartz, and D, San Carlos olivine are plotted against $\delta^{18}O$ values measured by manual and automated laser techniques. $\Delta^{17}O$ values are calculated from $\delta'^{17}O_{WST}$ and $\delta'^{18}O_{WST}$ values. Gray dashed lines represent zero deviation of $^{17}O/^{16}O$ ratio from the fractionation line. Error bars represent 1SEM [Color figure can be viewed at wileyonlinelibrary.com]

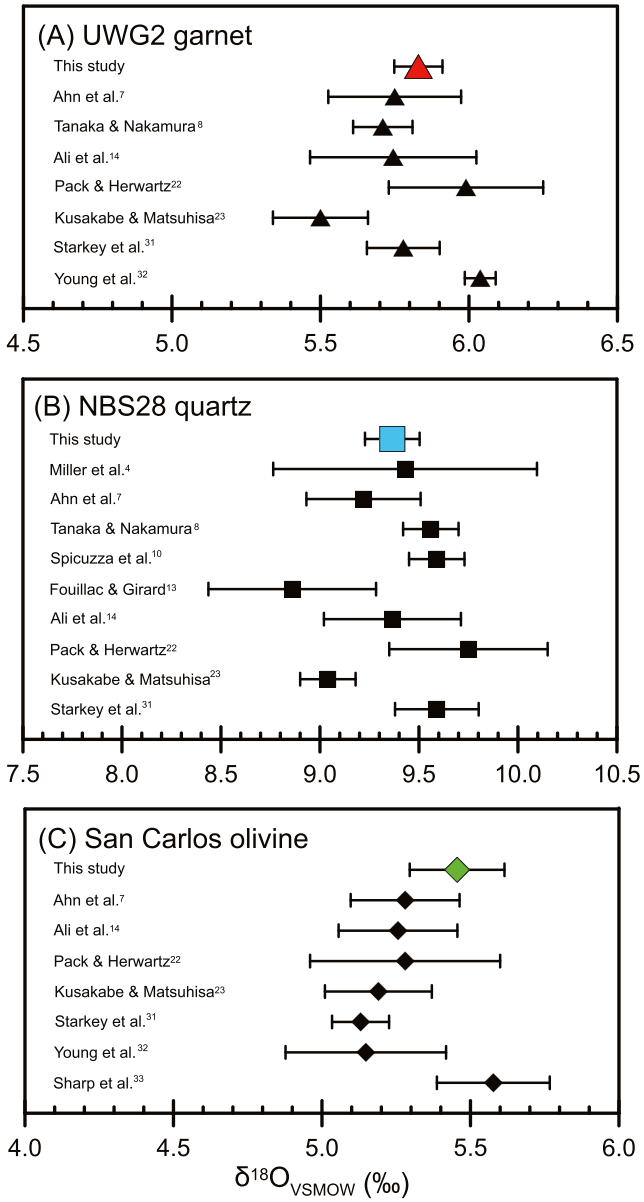

FIGURE 5 $\delta^{18}O_{VSMOW}$ values by the automated lasing technique of A, UWG2 garnet, B, NBS28 quartz, and C, San Carlos olivine obtained in this study. The data for NBS28 quartz and San Carlos olivine were obtained by automated method III because the high-density laser can prevent isotopic fractionation during laser fluorination. Literature data are shown for comparison. The error bars represent 2σ standard deviations [Color figure can be viewed at wileyonlinelibrary.com]

Depletion in ^{18}O is caused by the difficulty of breaking the Si-^{18}O bond at insufficient energy density, thus resulting in low $\delta^{18}O$ values.[9] In this respect, a high-density beam and rapid heating are recommended to avoid isotope fractionation during quartz fluorination.[8] As shown in Figure 3C, analysis with a high-density laser beam prevents isotope fractionation possibly caused by vaporization on the sample surface.[8-10] For San Carlos olivine (Figure 3D), the results obtained by automated mode III show slightly lower reproducibility ($\delta^{18}O_{WST}$ = 15.20 ± 0.16‰, n = 9) than the data obtained by the manual lasing technique. The fluorination products (e.g., MgF_2, FeF_2) which absorb infrared radiation could inhibit complete reaction resulting in detectable isotopic fractionation by partial reaction.[26,27] The results of NBS28 quartz and San Carlos olivine indicate that the isotopic fractionation appears to depend on the lasing technique used (Figures 3C and 3D). It is noted that the $\delta^{18}O$ values of the quartz and olivine samples increased with decreasing beam size (automated mode I → III). These results imply that the use of a high-density laser leads to unfractionated isotopic ratios. Moreover, isotopic fractionation of ^{17}O was also observed in the $\delta^{18}O$ versus $\Delta^{17}O$ plot (Figure 4). The $\Delta^{17}O$ values measured by the manual lasing technique are more scattered than the other data obtained by the automated lasing technique, except for the San Carlos olivine.

For comparison between the $\delta^{18}O$ values of the reference materials and literature data, $\delta^{18}O$ values relative to working standard O_2 are converted into the VSMOW scale by a conversion factor of 0.9904 (refer to Table S1, supporting information) using repetitive measurements of UWG2 garnet (n = 24) and assuming $\delta^{18}O_{VSMOW}$ = 5.8‰ for UWG2 garnet.[29] Figure 5 shows the $\delta^{18}O$ values of the reference materials obtained by the automated lasing technique and literature data obtained by the CO_2-laser fluorination method (see also Table S2, supporting information). The data for NBS28 quartz ($\delta^{18}O_{VSMOW}$ = 9.36‰, n = 10) and San Carlos olivine ($\delta^{18}O_{VSMOW}$ = 5.46‰, n = 9) were obtained by automated method III because a high-density laser can prevent isotopic fractionation during laser fluorination. The average $\delta^{18}O$ value of NBS28 quartz is slightly lower than the recommended value ($\delta^{18}O_{VSMOW}$ = 9.58‰),[30] but it is in good agreement with other literature data.[4,7,8,10,13,14,22,23,31] The average $\delta^{18}O$ value of San Carlos olivine is also in agreement with the margin of error of the literature data.[7,14,22,23,31-33] While it is still unclear why the isotopic variability of sample depends on the sample type and lasing technique, our results suggest that the automated laser control coupled by a defocused beam can provide satisfactory results with sufficiently high precision for the analysis of silicate minerals, and indicate that we can achieve good analytical reproducibility and minimize isotope fractionation by using the automated laser fluorination technique, i.e., rapid reaction with a high-density beam.

5 | CONCLUSIONS

We have measured the oxygen isotope compositions of reference minerals (UWG2 garnet, NBS28 quartz and San Carlos olivine) and in-house standards (MORB glass and obsidian). The system described herein enables us to measure the $\delta^{17}O$ and $\delta^{18}O$ values of silicate materials with high precision. The results obtained by the automated lasing technique show good reproducibility (2SD) of $\delta^{17}O$ and $\delta^{18}O$ values, which are ±0.06‰ and ±0.08‰ for UWG2 garnet, ±0.07‰ and ± 0.14‰ for NBS28 quartz, ±0.09‰ and ±0.16‰ for San Carlos olivine, ±0.10‰ and ±0.19‰ for MORB glass and ±0.08‰ and ±0.15‰ for obsidian. The $\Delta^{17}O$ values of samples also show high reproducibility (±0.02‰, 2SD). It is emphasized that the automated

lasing mode with a high-density beam and a short irradiation time leads to much better precision and unfractionated oxygen isotope compositions than the manual lasing mode.

ACKNOWLEDGEMENTS

The authors would like to thank the anonymous reviewers for their constructive comments that helped improve the manuscript. We also thank In-Seong Yoo, Sang Beom Park and Jong Min Baek for their technical support on improvements to the laser fluorination system and maintenance of the mass spectrometer in the Korea Polar Research Institute (KOPRI). This study was supported by KOPRI project PM18030 (20140409) and PE18110.

ORCID

Nak Kyu Kim https://orcid.org/0000-0002-2882-068X
Changkun Park https://orcid.org/0000-0002-1206-6803

REFERENCES

1. Clayton RN, Mayeda TK. The use of bromine pentafluoride in the extraction of oxygen from oxides and silicates for isotopic analysis. *Geochim Cosmochim Acta*. 1963;27(1):43-52.
2. Sharp ZD. A laser-based microanalytical method for the in situ determination of oxygen isotope ratios of silicates and oxides. *Geochim Cosmochim Acta*. 1990;54(5):1353-1357.
3. Elsenheimer D, Valley JW. In situ oxygen isotope analysis of feldspar and quartz by Nd: YAG laser microprobe. *Chem Geol*. 1992;101(1–2):21-42.
4. Miller MF, Franchi IA, Sexton AS, Pillinger CT. High precision $\delta^{17}O$ isotope measurements of oxygen from silicates and other oxides: Method and applications. *Rapid Commun Mass Spectrom*. 1999;13(13):1211-1217.
5. Kusakabe M, Maruyama S, Nakamura T, Yada T. CO_2 laser-BrF_5 fluorination technique for analysis of oxygen three isotopes of rocks and minerals. *J Mass Spectrom Soc Jpn*. 2004;52(4):205-212.
6. Pack A, Toulouse C, Przybilla R. Determination of oxygen triple isotope ratios of silicates without cryogenic separation of NF_3 – Technique with application to analyses of technical O_2 gas and meteorite classification. *Rapid Commun Mass Spectrom*. 2007;21(22):3721-3728.
7. Ahn I, Lee JI, Kusakabe M, Choi B-G. Oxygen isotope measurements of terrestrial silicates using a CO_2-laser BrF_5 fluorination technique and the slope of terrestrial fractionation line. *Geosci J*. 2012;16(1):7-16.
8. Tanaka R, Nakamura E. Determination of ^{17}O-excess of terrestrial silicate/oxide minerals with respect to Vienna standard mean ocean water (VSMOW). *Rapid Commun Mass Spectrom*. 2013;27(2):285-297.
9. Kirschner DL, Sharp ZD. Oxygen isotope analyses of fine-grained minerals and rocks using the laser-extraction technique. *Chem Geol*. 1997;137(1–2):109-115.
10. Spicuzza MJ, Valley JW, Kohn MJ, Girard JP, Fouillac AM. The rapid heating, defocused beam technique: A CO_2-laser-based method for highly precise and accurate determination of $\delta^{18}O$ values of quartz. *Chem Geol*. 1998;144(3–4):195-203.
11. Garlick GD, Epstein S. Oxygen isotope ratios in coexisting minerals of regionally metamorphosed rocks. *Geochim Cosmochim Acta*. 1967;31(2):181-214.
12. Rumble D, Farquhar J, Young E, Christensen C. In situ oxygen isotope analysis with an excimer laser using F_2 and BrF_5 reagents and O_2 gas as analyte. *Geochim Cosmochim Acta*. 1997;61(19):4229-4234.
13. Fouillac A-M, Girard J-P. Laser oxygen isotope analysis of silicate/oxide grain separates: Evidence for a grain size effect? *Chem Geol*. 1996;130(1–2):31-54.
14. Ali A, Jabeen I, Gregory D, Verish R, Banerjee NR. New triple oxygen isotope data of bulk and separated fractions from SNC meteorites: Evidence for mantle homogeneity of Mars. *Meteorit Planet Sci*. 2016;51(5):981-995.
15. Harju ER, Rubin AE, Ahn I, Choi B-G, Ziegler K, Wasson JT. Progressive aqueous alteration of CR carbonaceous chondrites. *Geochim Cosmochim Acta*. 2014;139:267-292.
16. Lee J-A, Kim K, Lee J-I, Choo M. Oxygen isotopic ratios for ultramafic xenoliths from the Korean peninsula. *J Korean Earth Sci Soc*. 2013;34(1):28-40.
17. Popova OP, Jenniskens P, Emel'yanenko V, et al. Chelyabinsk airburst, damage assessment, meteorite recovery, and characterization. *Science*. 2013;342(6162):1069-1073.
18. Miller MF. Isotopic fractionation and the quantification of ^{17}O anomalies in the oxygen three-isotope system: An appraisal and geochemical significance. *Geochim Cosmochim Acta*. 2002;66(11):1881-1889.
19. Levin NE, Raub TD, Dauphas N, Eiler JM. Triple oxygen isotope variations in sedimentary rocks. *Geochim Cosmochim Acta*. 2014;139:173-189.
20. Greenwood RC, Barrat J-A, Miller MF, et al. Oxygen isotopic evidence for accretion of Earth's water before a high-energy moon-forming giant impact. *Sci Adv*. 2018;4(3):eaao5928.
21. Spicuzza MJ, Day JM, Taylor LA, Valley JW. Oxygen isotope constraints on the origin and differentiation of the moon. *Earth Planet Sci Lett*. 2007;253(1–2):254-265.
22. Pack A, Herwartz D. The triple oxygen isotope composition of the earth mantle and understanding $\Delta^{17}O$ variations in terrestrial rocks and minerals. *Earth Planet Sci Lett*. 2014;390:138-145.
23. Kusakabe M, Matsuhisa Y. Oxygen three-isotope ratios of silicate reference materials determined by direct comparison with VSMOW-oxygen. *Geochem J*. 2008;42(4):309-317.
24. Eiler JM. Oxygen isotope variations of basaltic lavas and upper mantle rocks. *Rev Mineral Geochem*. 2001;43(1):319-364.
25. Young ED, Rumble D. The origin of correlated variations in in-situ $^{18}O^{16}O$ and elemental concentrations in metamorphic garnet from southeastern Vermont, USA. *Geochim Cosmochim Acta*. 1993;57(11):2585-2597.
26. Farquhar J, Rumble D. Comparison of oxygen isotope data obtained by laser fluorination of olivine with KrF excimer laser and CO_2 laser. *Geochim Cosmochim Acta*. 1998;62(18):3141-3149.
27. Wiechert U, Hoefs J. An excimer laser-based micro analytical preparation technique for in-situ oxygen isotope analysis of silicate and oxide minerals. *Geochim Cosmochim Acta*. 1995;59(19):4093-4101.
28. Ali A, Jabeen I, Banerjee NR, et al. The oxygen isotope compositions of olivine in main group (MG) pallasites: New measurements by adopting an improved laser fluorination approach. *Meteorit Planet Sci*. 2018;1-14.
29. Valley JW, Kitchen N, Kohn MJ, Niendorf CR, Spicuzza MJ. UWG-2, a garnet standard for oxygen isotope ratios: Strategies for high precision and accuracy with laser heating. *Geochim Cosmochim Acta*. 1995;59(24):5223-5231.
30. Gonfiantini R, Stichler W, Rozanski K. Standards and intercomparison materials distributed by the International Atomic Energy Agency for stable isotope measurements. IAEA-TECDOC-825. Vienna: IAEA; 1995.

31. Starkey NA, Jackson CR, Greenwood RC, et al. Triple oxygen isotopic composition of the high-$^{3}He/^{4}He$ mantle. *Geochim Cosmochim Acta*. 2016;176:227-238.
32. Young ED, Kohl IE, Warren PH, Rubie DC, Jacobson SA, Morbidelli A. Oxygen isotopic evidence for vigorous mixing during the moon-forming giant impact. *Science*. 2016;351(6272):493-496.
33. Sharp Z, Gibbons J, Maltsev O, et al. A calibration of the triple oxygen isotope fractionation in the SiO_2–H_2O system and applications to natural samples. *Geochim Cosmochim Acta*. 2016;186:105-119.

SUPPORTING INFORMATION

Additional supporting information may be found online in the Supporting Information section at the end of the article.

How to cite this article: Kim NK, Kusakabe M, Park C, et al. An automated laser fluorination technique for high-precision analysis of three oxygen isotopes in silicates. *Rapid Commun Mass Spectrom*. 2019;33:641-649. https://doi.org/10.1002/rcm.8389